

Solar image restoration by use of Multi-Object Multi-Frame Blind Deconvolution

Michiel van Noort, Luc Rouppe van der Voort

Institute of Theoretical Astrophysics, University of Oslo
P.O. Box 1029 Blindern, N-0315 Oslo, Norway
Center of Mathematics for Applications, University of Oslo
P.O. Box 1053 Blindern, N-0316 Oslo, Norway

Mats Löfdahl

Institute for Solar Physics of the Royal Swedish Academy of Sciences
AlbaNova University Center, SE-106 91 Stockholm, Sweden

Abstract. We present examples of the application of the image restoration method of Multi-Object Multi-Frame Blind Deconvolution to observations obtained with the Swedish 1-m Solar Telescope on La Palma. This restoration method is an extension of Joint Phase Diverse Speckle image restoration. Multiple realizations of multiple objects can now be restored jointly, facilitating near-perfect alignment between different objects. This greatly reduces false signals in the determination of derived quantities, such as magnetograms, Dopplergrams and Gband-continuum difference images.

1. Introduction

We present the application of the image restoration technique Multi-Object Multi-Frame Blind Deconvolution (MOMFBD, van Noort et al. 2005) to observations obtained with the Swedish 1-m Solar Telescope on La Palma. The goal is to obtain near diffraction-limited observations over a large field of view and over extended periods of time (>1 hour), bridging periods of bad seeing and removing residual aberrations not corrected by the Adaptive Optics (AO) system.

MOMFBD is an extension of the Multi-Frame Blind Deconvolution image restoration technique (MFBD, see e.g., Löfdahl 2002). Multiple realizations of multiple objects can now be restored jointly, e.g., series of simultaneously exposed G-band and continuum images, or series of broad-band and narrow-band images. The joint restoration of multiple image sets has the advantage that near-perfect alignment can be achieved between the different objects. This greatly reduces false signals in the determination of derived quantities, such as magnetograms, Dopplergrams, and G-band–G-cont difference images. The method is also advantageous for aligning images showing greatly varying solar scenes, e.g., narrow-band H α line core and continuum images.

The restoration of narrow-band images greatly benefits from joint processing with broad-band images. As the method requires short exposure times – to freeze the seeing – the signal-to-noise ratio in narrow band images can be very

low which would severely affect the restoration when processed separately. In combination with broad-band images, seeing effects are more effectively isolated from the restored images. In addition, by reducing many images jointly, the restored image maintains the photon statistics of the total number of accumulated photons in all the images combined.

2. Method

The MFBD method jointly estimates the un-aberrated object as well as the pupil phase aberrations responsible for the blurring in a Maximum Likelihood sense. A small number ($\lesssim 10$) of realizations of the random atmospheric turbulence is usually sufficient for good restorations. One of the basic assumptions is that the object (i.e., the solar image) is the same for all realizations. This limits the collection interval to $\lesssim 10$ s, the solar evolution time, assuming a sound speed on the Sun of ~ 7 km/s and a telescope resolution of $0''.1$.

MOMFBD is the parallel processing of several MFBD sets, subject to the constraint that the wavefront aberrations are identical for simultaneous exposures. The likelihood function of the MOMFBD problem is the sum of the likelihood functions of the individual MFBD sets and maximized by means of a gradient-search algorithm. The identical wavefronts are enforced in each maximization step by use of a Linear Equality Constraints (LEC) formalism, thus reducing the number of unknown wavefront parameters.

For example, application of the LECs from figure 1, together with pre-calculated local tilt components from a calibration step (see section 4.), ensures precise alignment of the narrow-band images to the broad-band images and thus of the narrow-band images to each other, even though the images are taken at separate instances in time. Subsequent data reduction steps can therefore assume that the images are well aligned (see figure 2).

3. Implementation

The implementation of the algorithm is coded in C++, which was found to be typically 30 times faster than the original implementation in ANA. The code makes use of the open source FFTW library (see URL: <http://www.fftw.org/>) for Fast Fourier transforms. To keep even very large problems manageable, the code is capable of using a large number of CPUs, connected with a network. CPUs can be added and removed at will and successful operation has thus far been achieved with more than 200 CPUs. For more information about the code and downloads, see URL: <http://www.momfbd.org/>

4. Observations

The observations were obtained with the Swedish 1-m Solar Telescope (SST, Scharmer *et al.* 2003a) on La Palma. The SST re-images the primary focus through a Schupmann system, that removes chromatic aberrations from the 1-m singlet lens. After the Schupmann focus follows a tip-tilt mirror, a deformable bimorph mirror, and a re-imaging lens that adapts the image scale to the cameras

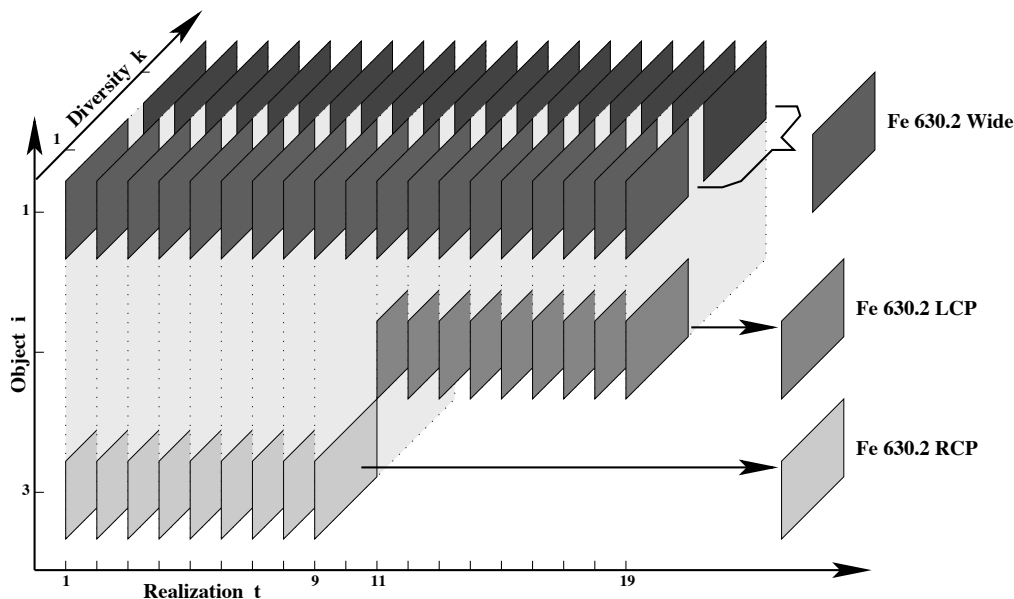


Figure 1. Linear equality constraints for the red beam setup. Simultaneous wavefront coefficients are constrained to be identical. Objects 2 and 3 (Fe I 6302 RCP and LCP) both do not have a diversity channel, they are aligned to object 1 (wide-band channel FWHM 8\AA centered on 6302\AA) and therefore to each other.

used. A dichroic beamsplitter ($\sim 5000\text{\AA}$) splits the light into a “red” and a “blue” beam. Both beams accommodate scientific cameras and the red beam also has the correlation tracker and a Shack–Hartmann sensor. The tip-tilt mirror, bimorph mirror (37 actuators), correlation tracker and Shack–Hartmann sensors constitute the SST AO system (Scharmer et al. 2003b).

Simultaneous exposure of the cameras is accomplished by use of an optical chopper. Typical exposure times were 10 ms for the blue beam and 15 ms for the red beam. For the red beam, only relatively fast MegaPlus 1.6 cameras were used and a frame rate of ~ 3.5 frames/s could be achieved. For the blue beam, the slower MegaPlus 4.2 cameras limited the frame rate resulting in an ~ 2.2 frames/s acquisition rate. These frame rates correspond to a data stream of 4.5–7 Mbytes/s which is written to the internal hard disks of the camera computers. The (compressed) raw data is stored to a separate raidset of hard disks during the night. For our August 2004 observing campaign, we operated 3 cameras on the red beam (SOUP and a broad-band phase-diversity (PD) pair) and 5 cameras on the blue beam (one PD pair for G-band, one PD pair for the continuum and one Ca H camera). The total amount of raw data collected during a 10 h observing day comprises 1.4 Tbytes. In practice, a typical observing day results in about 700 Gbytes.

Good image restoration requires sub-pixel alignment of all cameras. A pin-hole array was used to achieve a physical alignment to within 5 CCD pixels. Remaining offsets can be determined using the calibration mode of the MOMFBD program that estimates offsets from pinhole images. For the diversity cameras,

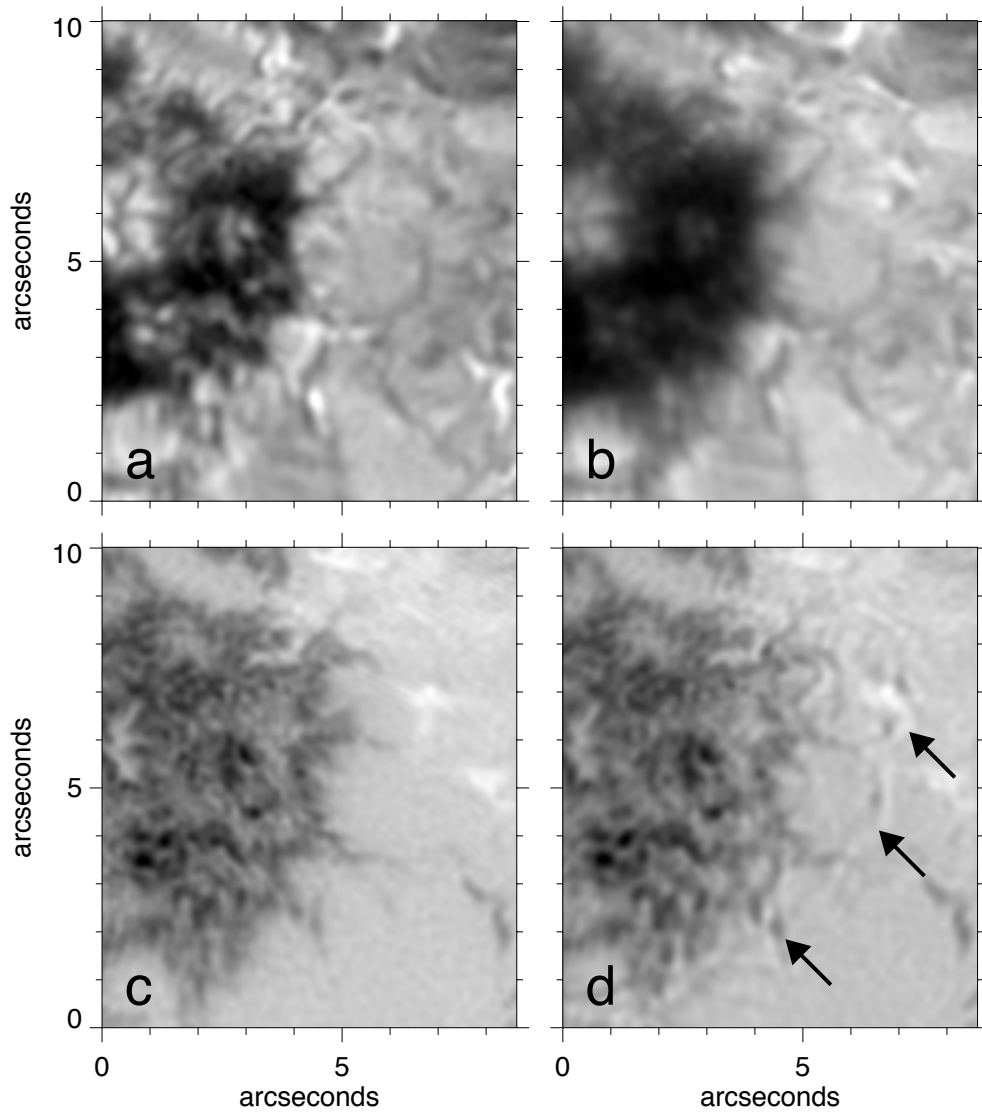


Figure 2. The bottom two panels show Fe I 6302 magnetograms made from -60 mÅ RCP and LCP images. The left panel (c) shows a magnetogram made from simultaneously restored RCP and LCP images. The right magnetogram (d) is made from separately restored RCP and LCP images which were aligned by sub-image cross-correlation and destretching. Arrows mark clear examples of spurious signals from alignment mismatches. The top two panels show the restored LCP (a) and RCP (b) images. Magnetic features have opposite color coding in the two polarization states: what is bright in LCP is dark in RCP and vice versa. Automatic alignment using cross-correlation is difficult in areas where magnetic signals are in close proximity to non-magnetic intensity gradients, like in the areas indicated by the top and bottom arrows. In fact, cross-correlation can create artifacts even in the absence of magnetic signal, as indicated by the center arrow.

the amount of de-focus is determined together with the tilt offsets. In this way it is also possible to remove other types of misalignments that can, to first order, be approximated by local translations, such as rotations and image scale differences, provided they are small.

5. Results

Figures 2 and 3 present results of MOMFBD processing of different data sets. Figure 2 compares a MOMFBD-processed FeI 6302 magnetogram with a magnetogram constructed from separately restored LCP and RCP images. The processing time of one magnetogram set, containing 18 narrow-band images (9 LCP, 9 RCP) and 2×19 broad-band images (focus and de-focus, see figure 1, amounts to about 75 CPU hours on a 3.2 GHz Pentium IV CPU with hyperthreading. To make the isoplanatic approximation valid, the images are divided into 19×12 sub-images of size 128×128 pixels ($\approx 6'' \times 6''$ undisturbed FOV) which are processed separately. Neighboring sub-images have ample overlap which allows for seamless mosaicking to make the final restored image.

Figure 3 shows a G-band image, an FeI 6302 magnetogram and a G-band–G-cont “magnetic” difference image. The processing time of one G-band/G-cont set, containing 2×10 G-band images (focus and de-focus) and 2×10 G-cont images (focus and de-focus), amounts to about 15 CPU hours.

More results from MOMFBD restored observations from our 2004 SST observing campaigns are presented in Rouppe van der Voort et al. (2006) in this volume.

Acknowledgments. This research was supported by the European Community’s Human Potential Programme through the European Solar Magnetism Network (ESMN, contract HPRN-CT-2002-00313), by The Research Council of Norway through grant 146467/420, through a grant of computing time from the Programme for Supercomputing, through a grant of computing time by participation in the CONDOR GRID computing project of the University of Oslo, and by the NSF under grant IIS ITR 03-24816. The Swedish 1-m Solar Telescope is operated on the island of La Palma by the Institute for Solar Physics of the Royal Swedish Academy of Sciences in the Spanish Observatorio del Roque de los Muchachos of the Instituto de Astrofísica de Canarias.

References

- Löfdahl, M. G. 2002, in *Image Reconstruction from Incomplete Data II*. eds. Bones, Fiddy, & Millane. Proc. SPIE, Vol. 4792, 146–155
- Rouppe van der Voort, L., van Noort, M., Carlsson, M., & Hansteen, V. 2006, in *ASP Conf. Ser.: Solar MHD: Theory and Observations - a High Spatial Resolution Perspective*, this volume
- Scharmer, G. B., Bjelksjö, K., Korhonen, T. K., Lindberg, B., & Petterson, B. 2003a, in *Innovative Telescopes and Instrumentation for Solar Astrophysics*. eds. S.L. Keil & S.V. Avakyan. Proc. SPIE., Vol. 4853, 341–350
- Scharmer, G. B., Dettori, P. M., Löfdahl, M. G., & Shand, M. 2003b, in *Innovative Telescopes and Instrumentation for Solar Astrophysics*. eds. S.L. Keil & S.V. Avakyan. Proc. SPIE., Vol. 4853, 370–380
- van Noort, M., Rouppe van der Voort, L., & Löfdahl, M. G. 2005, *Solar Phys.*, 228, 191

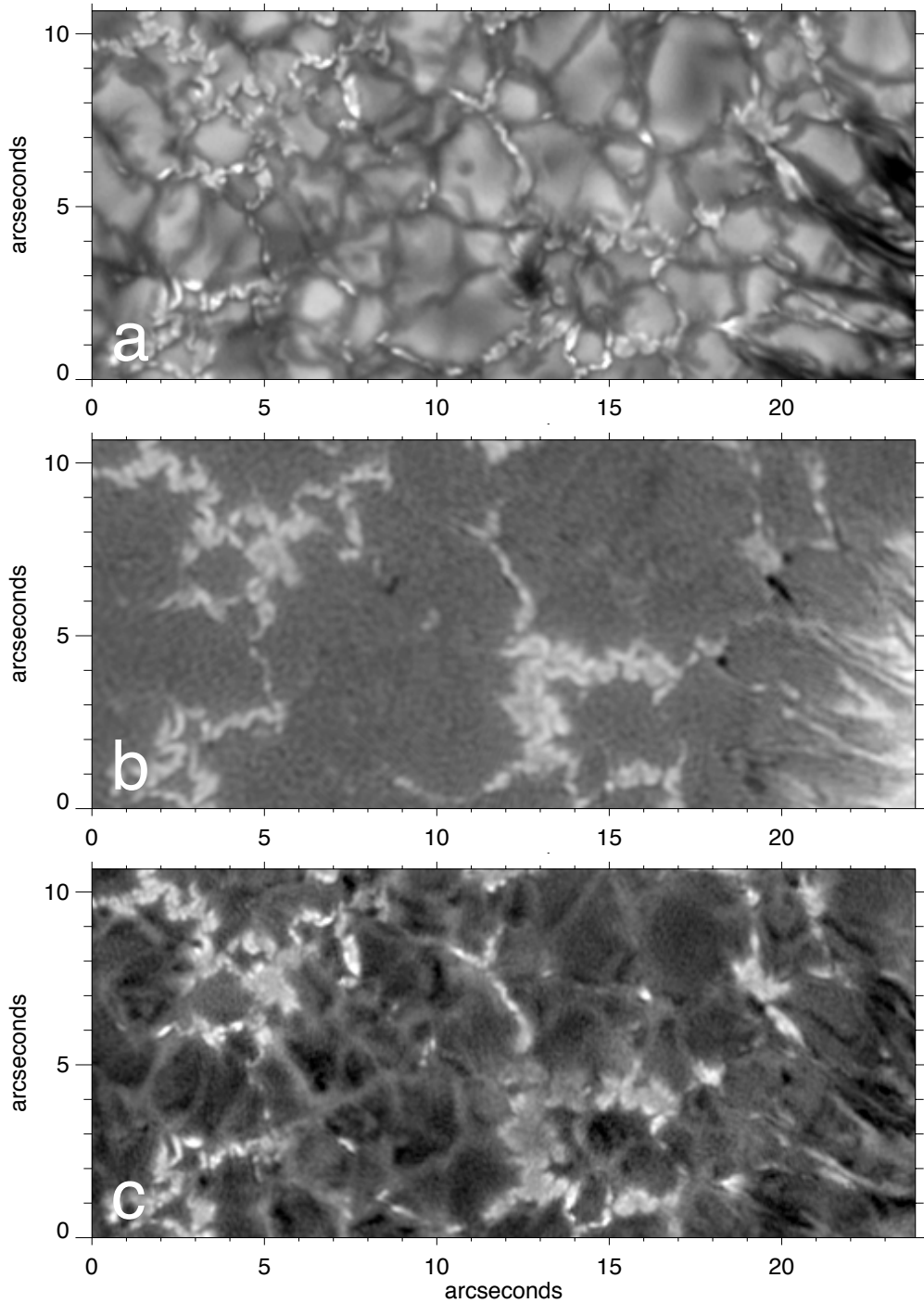


Figure 3. Close up of an area in the active region AR10662 observed with the SST on 21 August 2004 . **a:** G-band image. **b:** Fe I 6302 magnetogram. **c:** G-band–G-cont difference image. The G-band and G-cont images are jointly processed in a single MOMFBD restoration. The two resulting restored images are therefore perfectly aligned and the G-band–G-cont “magnetic” difference image is a simple subtraction which requires no further alignment. There is a clear correspondence between the brightest features in the difference image and the photospheric magnetic structures in the magnetogram.